Exploratory Tests of Hydrofoil Influence on Air Cavity under Model Boat Hull

Jeffrey M. Collins (V), **Konstantin I. Matveev** (V)
School of Mechanical and Materials Engineering, Washington State University, Pullman, WA

Significant frictional drag reduction of ships and boats can be achieved by forming extended air cavities underneath hulls. However, the air cavity benefit may degrade or disappear in off-design loadings and speed regimes, as well as in rough seas. To make this technology more viable, means for controlling the air-cavity properties are needed. One of promising compact devices that can alter the air-cavity shape and size is a hydrofoil. In this study, a hydrofoil-equipped model-scale boat with a bottom recess for holding air was tested under adverse loading conditions in a water channel. States with significant bow-up and bow-down trims, as well as a few heeled conditions, were produced by appropriately ballasting the hull. At these states, the air-cavity dimensions were substantially smaller than the hull recess. A hydrofoil mounted on side struts under the boat was shifted along the hull, and its effect on the air cavity length was recorded. The hydrofoil positions, corresponding to the longest cavities, were determined. Variations of the cavity length at different hydrofoil locations, sample photographs of the cavity boundaries, and investigated experimental conditions are reported in the paper. In addition, computational fluid dynamics simulations were initiated with the purpose to facilitate design of actuators for air-cavity flow control. A reasonably good agreement was found between experimental observations and numerical results. The present findings can help guide developments of compact hydrodynamic actuators for manipulating properties of air cavities under ship hulls.

KEY WORDS: Drag reduction; air-lubricated hulls; hydrofoil; flow control.

NOMENCLATURE

ACDR	Air cavity drag reduction
ALDR	Air-layer drag reduction
AoA	Angle of attack
BDR	Bubble drag reduction
L_c	Cavity length
L_h	Longitudinal position of hydrofoil
L_r	Length of hull recess
LCG	Longitudinal center of gravity
Sccs	Standard cubic centimeter per second

INTRODUCTION

Air lubrication of underwater hull surfaces is a promising method for reducing frictional ship drag, which can yield significant savings in required propulsive power. Effectiveness of this method is directly related to the total air layer coverage of submerged ship surfaces, which can be achieved by creating one or several air cavities, as shown in Fig. 1. An alternative method is to inject a stream of air bubbles along the hull, but it is not considered in this paper. The limited amount of experimental data and small scope of validated theoretical models for air-ventilated flows prevent confident scaling of experimental results to commercial applications. Previous research provides some insight into air cavity behavior under certain (mainly steady state) flow conditions but has not yet developed suitable methods to control the cavity across a range of ship attitudes that would likely be encountered in real world operation. This study explores the use of hydrofoils to influence air cavity characteristics at various trim and heel angles that mimic off-design operating conditions.

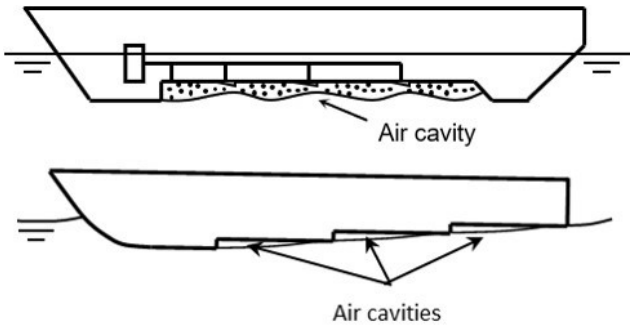

Fig. 1 Examples of air-cavity system application on marine vessels

Using air to reduce frictional drag on marine vessels was proposed at least as early as 1892 (Latorre, 1997), and interest in the subject has been renewed in recent years. Two primary differences have been identified by contemporary researchers to classify air lubrication systems; continuous injection of microbubbles into the boundary layers of submerged hull surfaces, often called “bubble” drag reduction (BDR), and formation of a continuous air cavity along significant portions of the hull area, referred to as “air cavity” drag reduction (ACDR) (Makiharju et al., 2012). Elbing et al. (2008) considered a concept of “air-layer” drag reduction (ALDR). Efforts by several

companies to commercialize air lubrication systems have largely focused on BDR techniques. Researchers in Japan retrofitted several sea ferries of various size with BDR injection systems that feature small hydrofoils near the air injection points, which use the suction side of the foil to reduce hydrostatic pressure and minimize required pumping work for the air supply (Kumagai et al., 2015). Over multiple trials, fuel savings ranged between 5-10%. Commercial implementations of ACDR systems have been less common than BDR, although previous efforts have demonstrated drag reduction up to 20% under certain operating conditions (Matveev et al., 2006).

Continuous air cavities have higher potential for energy savings due to larger air layer coverage with lower rates of air supply compared to ALDR and BDR, although commercial implementation of ACDR poses different challenges than BDR systems. Recessed regions in the hull are necessary to accommodate a stable air cavity, which is also affected by recess geometry at the leading and trailing edges in the water flow direction. Introducing a backward-facing step at the leading edge, as shown in Fig. 1, can induce natural cavitation to generate an air cavity at sufficiently high speeds, which can be augmented with additional air injection at lower speeds. The trailing portion of the recess must also be designed to minimize downstream convection of cavity air, which is often called a "beach" or "cavity locker." A gradual slope in this region is preferable to an abrupt step to avoid introducing additional water drag under conditions where the recess trailing edge is not sufficiently covered by the air cavity. Earlier experiments have shown the sloping beach reduces air loss in the water flow direction (Elbing et al., 2008), which in turn reduces the rate of air supply required to maintain a steady cavity. However, the total cavity length under the hull was found to decrease at sufficiently large (either positive or negative) angles of the hull trim (Matveev et al., 2009).

Comprehensive theoretical and numerical methods aimed at accurately modeling cavity behavior are still being developed. However, some global air-cavity metrics, such as the total cavity length, can be predicted even with 2D potential flow methods (Matveev et al., 2009). Similar models (Matveev, 2003; Matveev and Miller, 2011) suggest that the presence of a hydrofoil can have a favorable impact on air cavity characteristics. Hydrofoil effects were recently studied experimentally using a small model-scale structure, which was rigidly mounted in an aquarium with water flow provided by a small pump (Pace and Matveev, 2019). Changing the foil's longitudinal position, angle of attack and proximity to the air cavity surface showed significant impacts on the cavity shape. However, the preliminary results were limited in general applicability due to wall effects, non-uniform incident flow and the limited size of the test region.

The current study expands on hydrofoil experiments by using a larger hull model positioned in uniform water flow at higher speeds. To gain some preliminary data regarding the effects of hydrofoils on air cavities under more realistic conditions, the hull has been tested with various loading distributions, aiming specifically at off-design conditions with large trim angles. The experimental setup has also been modeled with a computational fluid dynamics (CFD) program under several simplifications. Simulations corresponding to experimental conditions produced air cavity flow regimes, including those affected by hydrofoils, in approximate agreement with experimental results, providing insight into modeling the air cavity behavior.

EXPERIMENTAL SETUP

Experiments with a model-scale air-cavity hull were conducted in an open-surface water channel at Washington State University. Facility schematics are shown in Fig. 2. Dimensions of the test section are 3.7 m x 0.9 m x 0.7 m. Water flow is driven by two pumps, with flow rate controlled using bypass valves to divert a portion of the water from the test section and through a recirculation circuit. Water velocity in the test section was measured by Pitot-static tubes and held between 52-56 cm/s during the test program, with a measurement accuracy of 1-4%. Earlier tests in the facility showed less than 2% variation of water velocity within the test section (Conger, 1992), which is comparable with the measurement uncertainty. The glass bottom and sides of the test section provide a full view of the flow region. Water depth during tests was maintained around 31 cm.

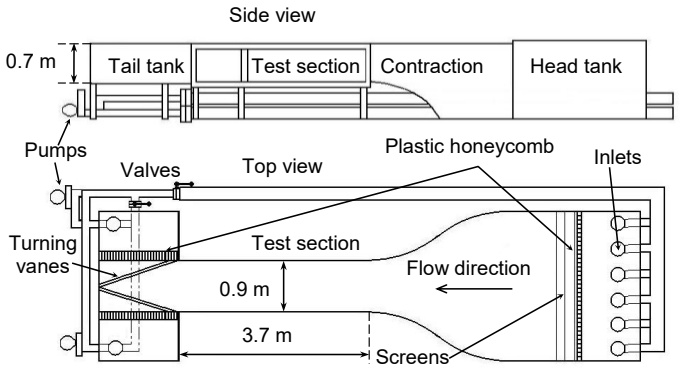

Fig. 2 Water channel schematic

The ship hull model was constructed from Styrofoam and covered with fiberglass to improve rigidity and surface properties. Relevant dimensions are shown in Fig. 3, and a photograph of the hull is given in Fig. 4. An acrylic plate was used as the cavity ceiling to observe characteristics of the air-water interface inside the recess. Air supply and cavity pressure measurements were conducted via two air taps on the cavity ceiling which had inner diameter 3 mm (Fig. 3). The rear portion of the cavity ceiling slopes downward at a 6° angle to act as a beach and minimize air leakage in the water flow direction without creating excessive pressure drag. At the cavity leading edge, a tab of length 65 mm and thickness 6.35 mm was installed. In the present tests, it was kept in the horizontal position along the bottom of the hull. To influence air layer characteristics, a 10-cm-chord hydrofoil of Eppler E603 profile was mounted beneath the air cavity with adjustable submergence, lengthwise position and angle of attack. A split hydrofoil of the same profile was used in additional tests with the tilted hull to influence air layer shapes that varied in the ship's beam-wise direction.

The unloaded model hull weighed about 6.4 kg with its corresponding longitudinal center of gravity (LCG) located 81 cm from the foremost point of the bow, as indicated in Fig. 3. Combined weight of the hydrofoil and its mounting apparatus was 0.9 kg. An additional 15.9 kg was added to the model during testing to increase hull submergence and make its weight more realistic for the given hull dimensions. Weight distribution along the hull was varied to achieve different trim and heel angles. Water surface elevations were measured at two longitudinal locations along the hull with permanently attached measuring tape, as were the cavity dimensions and the hydrofoil position.

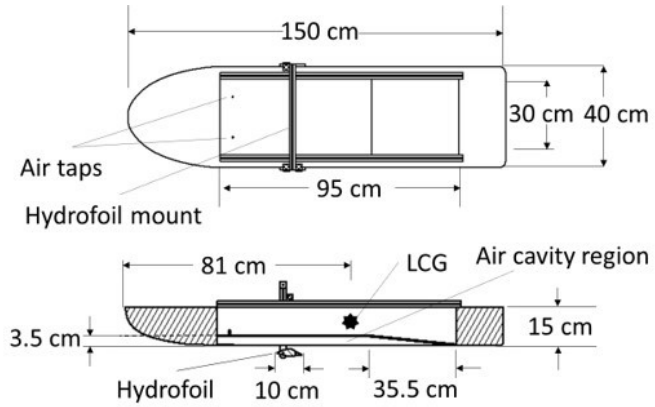

Fig. 3 Air-cavity hull features and main dimensions

Fig. 4 Photograph of the tested hull with hydrofoil visible under the hull

The hull was kept in the test section by means of a single fishing line connecting the bow to a rigid upstream fixture positioned above the water. This mounting arrangement allowed free adjustment of the hull's heave and pitch while the hull could undergo small motions in other degrees of freedom. In some conditions, attempts were made to measure drag force using a spring scale, but fluctuations and large uncertainty of this measurement precluded accurate reporting of drag values.

Air supply rates to the cavity region were measured using Dwyer RMA-1SSV and RMB-49-SSV rotameters with ranges of 3.9 and 15.75 standard cubic centimeters per second (sccs), respectively. Rotameter resolutions were 0.4 and 0.8 sccs, with reported accuracies within 2% of the full-scale range. A Dwyer Magnehelic differential pressure gage of range 500 Pa and resolution 12.5 Pa was used to monitor cavity pressure. Trim and heel angles were measured with a digital angle meter at an accuracy of 0.05°.

EXPERIMENTAL PROCEDURE

Tests were conducted with the hull ballasted to a mass of 23.2 kg. Three weight distributions were explored with LCGs at 72.0 cm, 77.6 cm, and 98.3 cm from the foremost point of the bow. These loadings resulted in trim angles of -2.5°, -0.6° and +2.5° at the operational speed of about 56 cm/s, which corresponded to a hull-length-based Froude number of about 0.15 and Reynolds number of about $7.5 \cdot 10^5$. A photograph of the ballasted hull with positive (bow-up) trim in the water channel is given in Fig. 5.

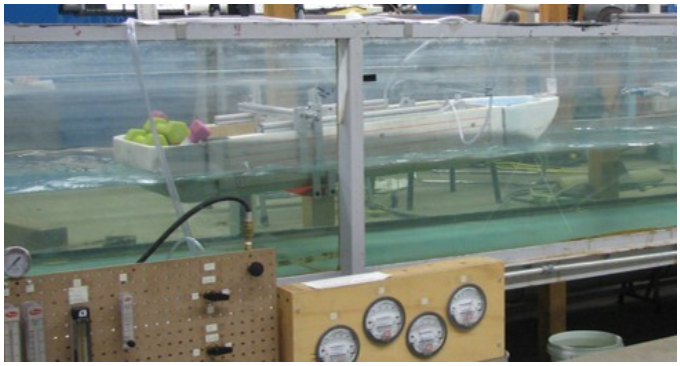

Fig. 5 Air-cavity hull tested in water channel

In all tests the air cavity was initially flooded with water, then a large air flow of about 20 sccs was supplied into the cavity. Several tests conducted with the low air supply from the beginning showed insignificant variation of the resulting steady state air-cavity properties. The time it takes to fill the recess with air can be roughly estimated as the ratio of the volume occupied by the air cavity in the steady state to the air supply rate, since only minimal air loss occurred during filling process in the present setup. After that, the initial air flow rate was reduced to 2.4 sccs, and upon reaching a steady state, measurements of the air-cavity properties were taken.

At near-zero trim conditions, the steady-state air cavity occupied nearly the entire bottom recess, so further improvement of the cavity with a hydrofoil was not warranted. However, at substantial trim angles (±2.5°), the area covered by the air was significantly smaller than the recess area. In these cases, a hydrofoil was employed beneath the hull to alter the air-cavity characteristics with the main objective being to increase its overall length.

Experiments were conducted with the hydrofoil positioned 1.35 cm below the hull baseplane (bottom of side skegs), and its angle of attack (AoA) was kept at a constant value of +5° in relation to the hull baseplane. The hydrofoil depth was selected to produce a significant effect on the air cavity while maintaining its complete submergence under the free water surface. At the relatively low flow velocities achievable in this water channel, changing the foil's AoA in the range of low (practically useful) angles had a relatively small impact on the cavity shape, and

therefore, the AoA was held constant. On the other hand, the hydrofoil longitudinal position was found to have pronounced effect on the air-cavity state, and hence, served as one of the main variables in this test series. The horizontal location of the hydrofoil is defined in Fig. 6.

Although some interesting dynamic phenomena were observed during the initial transient process when air fills the cavity, they were not a focus of this study and could not be accurately characterized with capabilities of the present setup. Hence, only steady-state regimes were quantified and reported. Approximate values for total drag forces ranged from 1.5 to 3.5 N in different conditions. As noted earlier, the model was allowed to undergo small motions in various degrees of freedom, which led to significant measured drag fluctuations of about 0.5-1 N and prevented accurate reporting of drag measurements. At low and positive trim angles, cavity pressure approximately corresponded to hydrostatic pressure at the water free surface in the cavity recess, typically 500-750 Pa with noticeable fluctuations. Negative trim angles sometimes caused water to cover the pressure tap and prevented such measurements.

Small motions of the hull in previously mentioned degrees of freedom also caused fluctuations of around ±2 cm in the cavity length. Average values for cavity length were recorded after fluctuation magnitudes became steady and repeatable for several minutes.

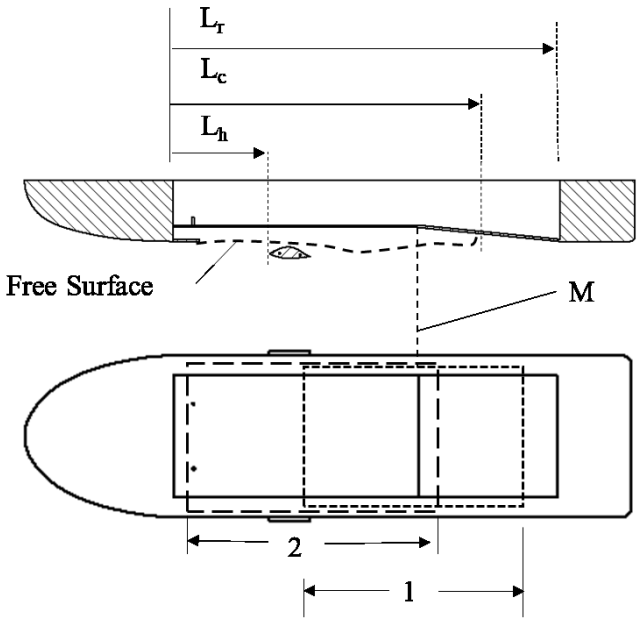

Fig. 6 Definition of the hydrofoil location, L_h, cavity length, L_c, recess length, L_r, and the front sloping section marker, M. Recess regions 1 and 2 (shown by dashed boxes on the bottom sub-figure) correspond to top-view photographs shown in Figs. 7 and 9.

RESULTS

The maximum possible air layer length based on the bottom recess geometry is L_r = 95 cm, as shown in Figs. 3 and 6. At near-zero trim values and zero heel, hydrostatic pressure at the free water surface inside the recess is nearly constant along the cavity length, allowing full development of the air cavity in the water flow direction (Fig. 7a). The sloping surface ("beach") in the rear portion of the cavity ceiling is rather effective in this loading condition and minimizes air leakage from the cavity. Even when air supply to the cavity was eliminated, air layer size reduced only slightly in the beginning and remained nearly constant over time at around 93 cm.

To imitate off-design ship loading conditions, trim angles of ±2.5° were induced on the model hull by re-distributing ballast weights. As the trim angle increased in either direction, the air layer length decreased, as shown in Fig. 7b,c and schematically illustrated in Fig. 8.

Negative trim angles allowed for a longer air layer, but also diminished effects of the sloping beach and allowed air to escape more freely from the cavity tail. At this loading condition, hydrostatic pressure decreased in the water flow direction along the hull and led the appearance of the wet area on the ceiling in the front part of the cavity (Fig. 7b). Near this region, the air layer could not stabilize because the pressure gradient forced downstream convection of supplied air, although a small area on the cavity ceiling near air injectors remained dry. At the positive trim angle, air was forced to escape under the cavity sidewalls before it could propagate behind the flat ceiling portion (Fig. 7c). At this loading condition, hydrostatic pressure on the hull increases in the direction of water flow and limits growth of the air layer.

At all trim conditions, increasing the heel angle from zero to 3.7° reduced the total air layer coverage, and negative trim angles showed the highest sensitivity to heeling. For near-zero and positive trim angles (Fig. 7d,f), the effects of heel angle on the air layer boundary were almost anti-symmetric with respect to the hull centerplane. At the negative trim, increasing the heel resulted in wetted regions at both the front and rear portions of the air cavity (Fig. 7e).

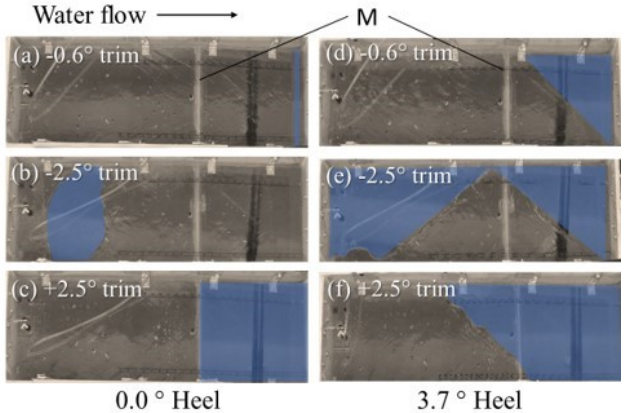

Fig. 7 Top view on air cavity shapes at different trim and heel angles. Blue-shaded areas show wetted ceiling areas. M indicates the sloping section marker defined in Fig. 6.

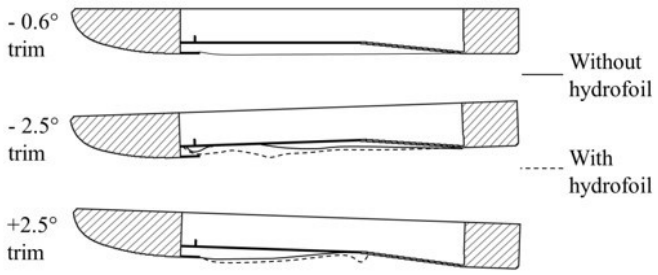

Fig. 8 Approximate air cavity shapes at various trim angles: solid curve, without hydrofoil; dashed curve, with hydrofoil at large trim magnitudes.

To determine whether the air-cavity areas could be altered in adverse hull loading conditions with substantial trim angles, a hydrofoil was placed under the hull, and its horizontal position was adjusted with the purpose of increasing cavity size. Influence of the hydrofoil on air layer at zero heel angles is shown in Fig 9. Under the negative trim condition (Fig. 9d-f), the optimal positioning of the hydrofoil at L_h/L_r = 0.08 allowed the air layer to cover almost the entire recess region and eliminated the wetted area that was present in the absence of hydrofoil (Fig. 7b). The total resulting cavity length was equal to that achieved at low trim angles (even without hydrofoil). The local drop in pressure around the top surface of the hydrofoil was sufficient to overcome hydrostatic pressure gradient in the wetted region, which had previously forced downstream convection of supplied air and prevented stabilization of the extended air cavity.

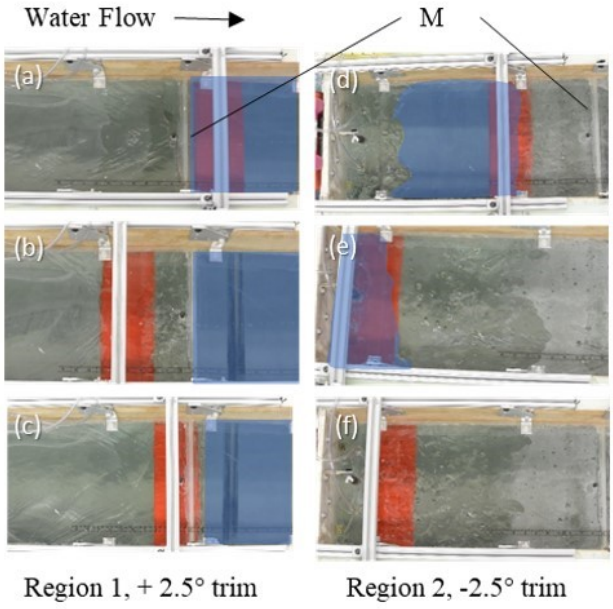

Fig. 9 Air cavity shapes with influence of hydrofoil (painted in red). Regions 1 and 2 correspond to the boxed areas defined in Fig. 6. Wetted areas without a sustained air layer are blue-shaded. M shows the sloping section marker defined in Fig. 6.

At positive trim angles the hydrofoil had a much smaller impact on air layer length, as the local pressure drop was insufficient to grow the air layer significantly. Further reductions in local pressure at the front part of the beach would be necessary to extend the air layer downstream and reduce leakage under the cavity sidewalls. This can be likely achieved with the boat operating at higher speeds when pressure modifications caused by a hydrofoil will be more prominent.

The effect of the hydrofoil on the cavity length depends on the foil's longitudinal position, as observed in Fig. 7 and 9. The quantitative information about the overall air-cavity length dependence on the foil location at large trim angles and zero heel is given in Fig. 10. In all cases, moving the foil more than 5% away from its optimal location diminishes benefits substantially. The maximum air layer length for negative trim was achieved with the foil located at L_h/L_r = 0.08 from the leading cavity edge. At around L_h/L_r = 0.1, the foil increases air leakage in the water flow direction and decreases total cavity length below what was achieved without a foil. At positive trim angles, the effects are less pronounced, as the total cavity length benefits relatively little from the hydrofoil at this loading condition and the low speed studied. However, the maximum air-cavity is still noticed at L_h/L_r = 0.58.

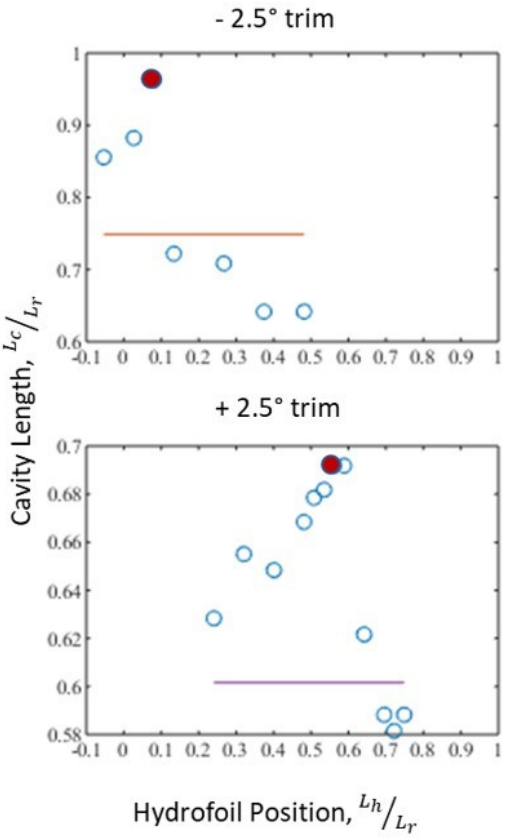

Fig. 10 Change in the cavity length at various longitudinal positions of hydrofoil for two significant trim angles. Circles correspond to data in setups with hydrofoil; horizontal lines, cavity length without hydrofoil. Filled in circles represent maximum cavity lengths.

When a ship hull exhibits a significant heel, one could be motivated to use a split hydrofoil to exert different effects on the air cavity at the port and starboard sides of the hull. Only brief qualitative tests with a such a hydrofoil were carried out in this study. The general aims were to reduce beam-wise variations of the cavity boundaries (e.g., to make the cavity more uniform) and to enlarge the cavity area whenever possible. The cavity areas influenced by a split foil are shown in Fig. 11d-f. The split foil allows control over local pressure near the air-water interface, which enables additional influence over total air layer coverage. Although exact changes in air layer size were not quantified in relation to hydrofoil positions, the observed modifications suggest that the beam-wise air-cavity control, although less effective, is also possible.

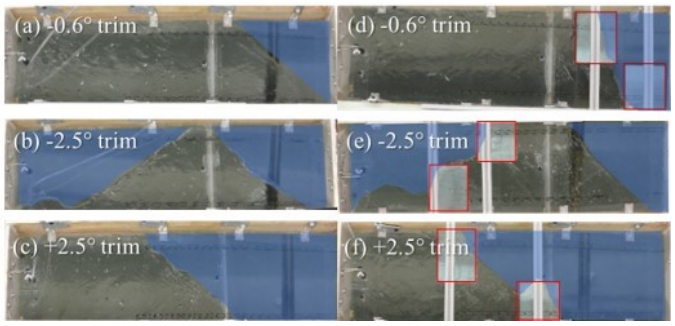

Fig. 11 Influence of split hydrofoil arrangement on air layer shape at a heel angle of 3.7°. Left, without hydrofoil; right, with hydrofoil. Water flow is from left to right. Hydrofoil borders highlighted for clarity.

NUMERICAL MODELING

To provide more insight on fluid mechanics phenomena observed in the present experiments and move towards developing high-fidelity modeling tools for design of controlled air-cavity systems, numerical modeling was started in this work. A computational fluid dynamics (CFD) software Star-CCM+, often used in marine engineering, was chosen for this study. This program employs a finite-volume viscous solver for fluid flow. The second-order discretization in space and the first-order stepping in time were utilized. The volume-of-fluid (VOF) method was used to resolve the air-water interface. The RANS approach employing a realizable $k-\varepsilon$ turbulence model was selected, which is generally recommended as an economical setting for modeling free-surface flows (Matveev et al., 2019). The surface tension was also activated.

Due to a constrained project timeline and limited computational resources, several simplifications were made in the CFD study. Only a few cases were simulated with the primary goal to see whether a qualitative agreement with test data can be achieved. Only two-dimensional configurations were considered using the centerplane hull geometry. Four setups were analyzed: ±2.5° fixed-trim, zero-heel hulls without the hydrofoil and with the hydrofoil at its optimal positions. These positions were assigned as L_h/L_r = 0.58 for the positive trim and L_h/L_r = 0.08 for the negative trim.

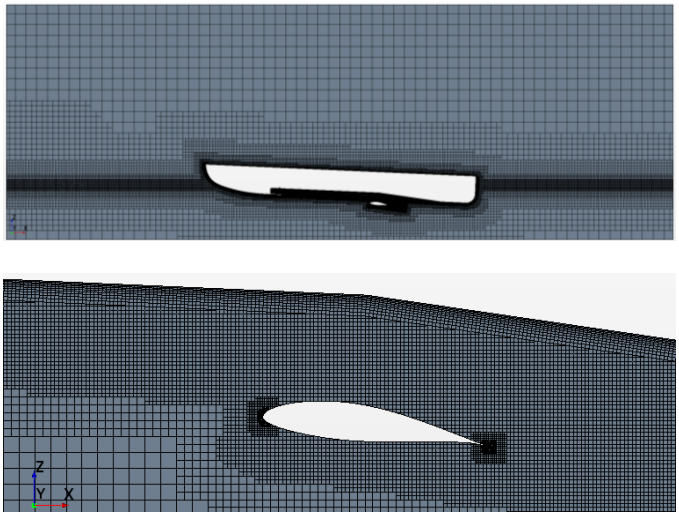

Fig. 12 Numerical mesh for the bow-up hull with hydrofoil in the entire domain (top) and around hydrofoil (bottom).

The numerical mesh was constructed with dense regions near the hull, including the bottom recess and hydrofoil, as well as along the free water surface in front of and behind the hull (Fig. 12). The experimental hull submergences were used to assign the hull vertical position. The incident water flow of 56 cm/s was specified at the upstream boundary of the numerical domain, while the hydrostatic pressure distribution was used at the outlet. The bottom and top boundaries of the domain were treated as slip walls, and the air was assumed to be stagnant at the upstream boundary above the hull (since there was no incident external airflow in the experiment). The solid hull surface was treated as a no-slip wall. The two-dimensional mass flow rate of air to the bottom recess was selected as 0.04 g/(m·s).

Following the procedure for estimating numerical uncertainty, simulations were conducted using three mesh levels (fine, medium and coarse). With use of Richardson extrapolation (Ferziger and Peric, 1999) and the factor of safety (Roache, 1998), the numerical uncertainty for the air-cavity length was estimated as 2.8%. The cell counts of fine two-dimensional grids in this study were about 50 thousand.

The simulations were started with the water-flooded bottom recess. High values of air flow rate were applied in the beginning to quickly generate a large air cavity (similar to experiments). Then, the air supply was reduced, and the flow was allowed to settle into a quasi-steady regime, when the time-averaged flow properties stopped evolving.

Solutions corresponding to steady states are illustrated in Figs. 13-14 for the volume fraction of water. Despite simplifications in the numerical setup, similarities to experimental observations are apparent. Without the hydrofoil, the air cavity stops around the end of the horizontal ceiling of the bottom recess in case of the bow-up hull (Fig. 13), whereas there is unsteady, partly wetted zone in the forward part of the recess when the hull is in the bow-down state (Fig. 14). The addition of the hydrofoil moves the air-

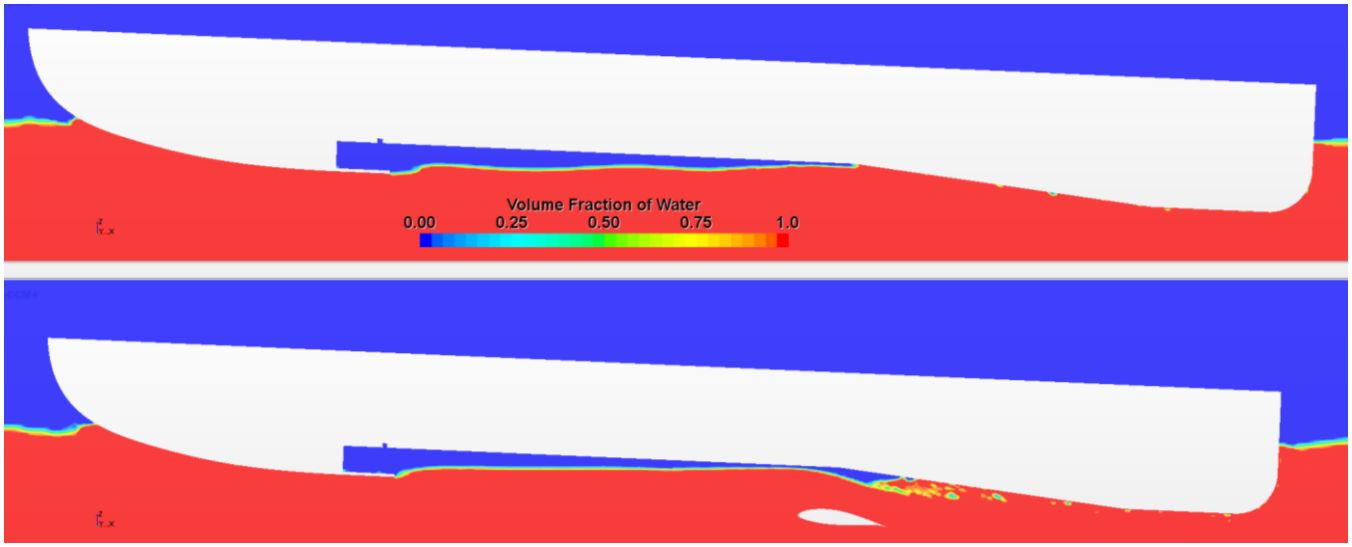

Fig. 13 Water volume fractions for bow-up hull: top, without hydrofoil; bottom, with hydrofoil.

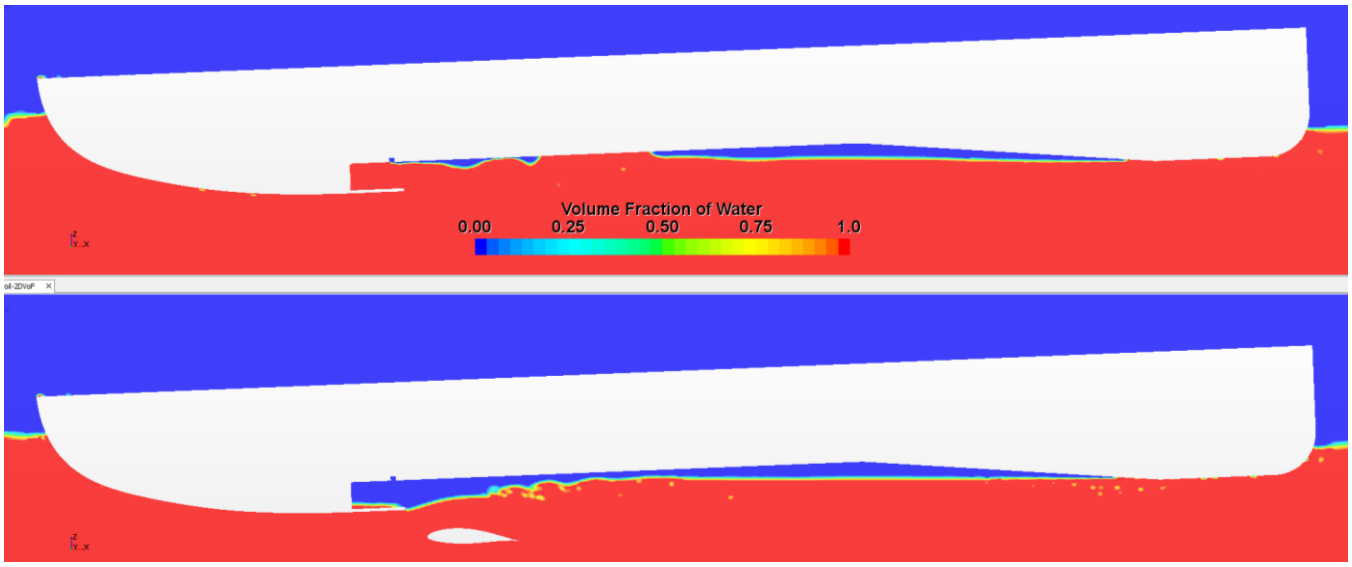

Fig. 14 Water volume fractions for bow-down hull: top, without hydrofoil; bottom, with hydrofoil.

cavity reattachment further downstream for the bow-up hull (Fig. 13), whereas the front part of the air cavity becomes much thicker in the bow-down case (Fig. 14).

While the hydrofoil certainly makes the air cavities occupy larger hull surface area, it also roughens the cavity surface above the foil tail and affects the way air sheds from the cavity. The hydrofoil influence on the air-cavity elongation is mainly due to acceleration of the water flow and decrease of pressure above the hydrofoil. This helps bring and retain more air, thus making air cavities bulkier in that zone. However, in the bow-up case the increased pressure upstream of the hydrofoil makes the cavity thinner (Fig. 13) which may lead to easier disintegration the air cavity upon a significant disturbance that likely happens when the foil is moved further downstream (Fig. 10). Optimizing the hydrofoil shape and its location may help reduce this unsteadiness and thus the air leakage, and therefore, may lead to further increase of the cavity size at the same air supply.

CONCLUSIONS

Exploratory tests were conducted with a model-scale hull in a water channel to establish effects of a hydrofoil on the air cavity properties in conditions with large trim angles of the hull. It was found that a hydrofoil can increase the cavity length when it is positioned near the cavity tail in the bow-up case and near the cavity front in the bow-down situation. With more forward placement of a hydrofoil, its effectiveness decreases, while the rearward shift leads to shorter cavities. In the heeled states, a split

hydrofoil was found to affect the cavity area as well but to lesser effect. Simplified CFD modeling produced a reasonable agreement with experimental findings, thus showing a promise to use numerical simulations for initial optimization studies.

Since the hydrofoil exerts a positive influence on the cavity size, this and other compact actuators (tabs, spoilers) should be investigated further in broader speed range and in the presence of waves to determine whether these elements can maximize drag-reducing performance of air cavities. The actuators of this sort may accelerate implementation of the air-cavity technology and thus improve sustainability of the maritime industry.

It can be noted that there was no single position of a hydrofoil in the investigated setup that could produce benefit for all trim and heel angles. With additional variations in operational conditions, such as speeds and sea states, it is likely that a system controlling hydrofoils or other actuators must be made adaptive to ensure effectiveness of actuator influence on air cavities in different regimes.

ACKNOWLEDGEMENTS
This material is based upon work supported by the National Science Foundation under Grant No. 1800135.

REFERENCES
Conger, R.N. *Pressure Measurements on a Pitching Airfoil in a Water Channel.* MS Thesis, Washington State University, Pullman, WA, 1992.

Elbing, B.R., Winkel, E.S., Lay, K.A., Ceccio, S.L., and Perlin, M. "Bubble-Induced Skin-Friction Drag Reduction and the Abrupt Transition to Air-Layer Drag Reduction." *Journal of Fluid Mechanics,* 612 (2008): 201-236.

Ferziger, J.H. and Peric, M. *Computational Methods for Fluid Dynamics*. Berlin: Springer, 1999.

Kumagai, I., Takahashi, Y., and Murai, Y. "Power Saving Device for Air Bubble Generation Using a Hydrofoil: Theory, Experiments, and Application to Ships." *Ocean Engineering,* 95 (2015): 183-194.

Latorre, R. "Ship Hull Drag Reduction Using Bottom Air Injection." *Ocean Engineering*, 24:2 (1997): 161-175.

Makiharju, S.A., Perlin, M., and Ceccio, S.L. "On the Energy Economics of Air Lubrication Drag Reduction." *International Journal of Naval Architecture and Ocean Engineering,* 4 (2012): 412-422.

Matveev, K.I. "On the Limiting Parameters of Artificial Cavitation." Ocean Engineering, 30:9 (2003): 1179-1190.

Matveev, K.I., Duncan, R., and Winkler, J., "Acoustic, Dynamic, and Hydrodynamic Aspects of Air-Lubricated Hulls," *Proceedings of Undersea Defense Technology Conference*, San Diego, CA, 2006.

Matveev, K.I., Burnett, T.J., and Ockfen, A.E. "Study of Air-Ventilated Cavity under Model Hull on Water Surface." *Ocean Engineering,* 36 (2009): 930-940.

Matveev, K.I. and Miller, M.J. "Air Cavity with Variable Length under a Model Hull." *Proceedings of the Institution of Mechanical Engineers, Part M: Journal of Engineering for the Maritime Environment,* 225:2 (2011): 161-169.

Matveev, K.I., Wheeler, M.P., and Xing, T. "Numerical Simulation of Air Ventilation and Its Suppression on Inclined Surface-Piercing Hydrofoils." *Ocean Engineering*, 175 (2019): 251-261.

Pace, M.V. and Matveev, K.I., "Modification of Air Cavity Flow under Model Hull with Hydrodynamic Actuators," *Proceedings of ASME-JSME-KSME Fluids Engineering Conference*, San Francisco, CA, ASME paper AJKFLUIDS2019-4632, 2019.

Roache, P.J. *Verification and Validation in Computational Science and Engineering*. Albuquerque: Hermosa, 1998.